Marine reservoir ages for coastal West Africa

Guillaume Soulet[1], Philippe Maestrati[2], Serge Gofas[2,3], Germain Bayon[1], Fabien Dewilde[1], Maylis Labonne[4], Bernard Dennielou[1], Franck Ferraton[4], Giuseppe Siani[5]

1 Ifremer, Univ Brest, CNRS, Geo-Ocean UMR6538, F-29280, Plouzané, France
2 Muséum National d'Histoire Naturelle, Paris, DGD-Collections, France
3 Departamento de Biología Animal, Facultad de Ciencias, Universidad de Málaga, Málaga, Spain
4 MARBEC, Univ Montpellier, CNRS, Ifremer, IRD, Montpellier, France
5 GEOPS, UMR 8148 Université Paris-Saclay, Orsay, France

Correspondence to: Guillaume Soulet (gsoulet@ifremer.fr)

Abstract. We measured the ^{14}C age of pre-bomb suspension-feeding bivalves of known age from coastal West Africa across a latitudinal transect extending from 33°N to 15°S. The specimens are from collections belonging to the Muséum National d'Histoire Naturelle (Paris, France). They were carefully chosen to ensure that the specimens were collected alive or died not long before collection. From the ^{14}C-dating of the known-age bivalves, we calculated the marine reservoir age (as ΔR and R values) for each specimen. ΔR values were calculated relative to the Marine20 calibration curve and the R values relative to Intcal20 or SHcal20 calibration curves. Except for five outliers, the ΔR and R values were generally homogenous with a weighted mean value of -72 ± 42 ^{14}C yrs (1sd, n = 24), and 406 ± 56 ^{14}C yrs (1sd, n = 24), respectively. These values are typical of low-latitude marine reservoir age values. Five suspension-feeding species living in five different ecological habitats were studied. For localities where several species were available, the results yielded similar results whatever the species considered, suggesting that in these locations the habitat has only a limited impact on marine reservoir age reconstruction. We show that our measured marine reservoir ages follow the declining trend of the global marine reservoir age starting ca. 1900 AD, suggesting that the marine reservoir age of coastal West Africa is driven, at least to first order, by the atmospheric CO_2 ^{14}C ageing due to fossil fuel burning rather than by local effects. Each outlier was discussed. Local upwelling conditions or sub-fossil specimens may explain the older ^{14}C age and thus larger marine reservoir ages for these samples. *Bucardium ringens* might not be the best choice for marine reservoir age reconstructions.

1 Introduction

The marine reservoir age (R) at a given calendar date/year (t) is the difference between the radiocarbon age (^{14}C) of the dissolved inorganic carbon (DIC) of the ocean ($^{14}C_m$) and that of atmospheric CO_2 ($^{14}C_{atm}$) (Stuiver et al., 1986; Stuiver and Braziunas, 1993)(Ascough et al., 2005; Soulet et al., 2016; Skinner and Bard, 2022):

$$R(t) = {}^{14}C_m(t) - {}^{14}C_{atm}(t) \quad (1)$$

At global scale, the marine reservoir age of the surface mixed layer of the ocean is set by the exchange of "young" CO_2 at the atmosphere-ocean interface, plus the exchange of DIC between oceanic surface waters and deep waters that contain large amounts of "old" DIC (Bard, 1988; Skinner and Bard, 2022). Box models have been used to study the distribution of radiocarbon in Earth's system since the 1950s (Craig, 1957; Revelle and Suess, 1957; Arnold and Anderson, 1957; Siegenthaler, 1983). The ^{14}C age of the global ocean over time, i.e. the Marine20 calibration curve (Heaton et al., 2020), has been modelled using the global carbon cycle box model BICYCLE (Köhler et al., 2006; Köhler and Fischer, 2006, 2004; Köhler et al., 2005) and the Northern Hemisphere atmospheric ^{14}C calibration curve (IntCal20; Reimer et al., 2020). While the global marine calibration curve (Marine20) is widely used to derive calibrated ages from ^{14}C dating of marine samples, it does not account for local marine ^{14}C offsets due to, for instance, continental carbon inputs to the coastal ocean, regional winds, and changes in the oceanic circulation and climate (Bard, 1988; Alves et al., 2018; Skinner and Bard, 2022; Heaton et al., 2023). Hence the importance of the metric ΔR (Stuiver et al., 1986; Stuiver and Braziunas, 1993; Reimer and Reimer, 2017), that is, the difference between the ^{14}C age of any marine sample ($^{14}C_m$) and that of the marine calibration curve ($^{14}C_{Marine20}$) at the same time (t):

$$\Delta R(t) = {}^{14}C_m(t) - {}^{14}C_{Marine20}(t) \quad (2)$$

The local marine reservoir age offset (ΔR) is known to vary greatly as demonstrated by pre-bomb values ranging between – 500 to + 2000 ^{14}C years (Reimer and Reimer, 2001) depending on the location. Most larger ΔR values are located at high-latitudes while values close to ΔR = 0 ^{14}C years are located at low latitudes (Bard, 1988; Bard et al., 1994).

From a geochronological perspective (i.e., calibration of marine ^{14}C dates and building age-depth models from marine ^{14}C dates), knowing the ΔR(t) is of crucial interest to correct marine ^{14}C dates for a local ^{14}C offset compared to the global marine calibration curve and hence prerequisite to derive accurate calendar ages. Reconstructing ΔR(t) values from unstudied areas is also valuable as it could contribute to deriving regional/local marine calibration curves from the global one using a 3-D large-scale ocean circulation model (Butzin et al., 2017; Alves et al., 2019).

From a carbon cycle perspective, the R(t) and ΔR(t) are also important as they reflect ^{14}C disequilibria between the ocean and the atmosphere and hence are key proxies to understand local variations of the global carbon cycle, and its evolution over time with the changing climate and environment (Skinner et al., 2015, 2010; Lindsay et al., 2016; Soulet et al., 2011; Siani et al., 2001; Schefuß et al., 2016; Heaton et al., 2021).

The estimation of R(t) and ΔR(t) values wherever possible is conducive to understanding modern and past carbon cycles, and the reconstruction of climate and environmental changes based on sedimentary archives.

Pre-bomb R(t) and ΔR(t) values for coastal West Africa are very sparse. According to the Marine Reservoir Correction Database (Reimer and Reimer, 2001; http://calib.org/marine/; last seen 15/11/2022), from Oran on the Mediterranean coast of Algeria (Siani et al., 2000) to Hondelkip Bay on the Atlantic coast of South Africa (Dewar et al., 2012), only a few marine reservoir ages from Mauritania and Senegal were reported (Ndeye, 2008) (Fig. 1). For Mauritania, the collection sites were Nouadhibou (formerly Port-Étienne, two samples), and the area of Cape Timiris – El Mamghar (three samples). Two samples were collected from an unknown location from coastal Mauritania. For Senegal, collection sites were restricted to the Dakar area (Almadies, Dakar harbour, Gorée Island and Rufisque; five samples). Thirteen additional samples were from unknown locations from coastal Senegal.

In this study we report new marine reservoir age values (n=30) based on the ^{14}C dating of bivalves with a known pre-bomb collection date and collected across a latitudinal transect extending from Mohammedia (Morocco, 33°N) to Moçâmedes (Angola, 15°S). Our suite of samples includes specimens from Mauritania, Senegal, Republic of Guinea, Sierra Leone, Ivory Coast, Benin, Gabon and Republic of Congo (Fig. 1, Table S1 in the Supplement). We used specimens of five different species: *Senilia senilis*, *Bucardium ringens*, *Donax rugosus*, *Ostrea stentina* and *Pseudochama gryphina*. We briefly discuss our results in the context of the local environmental setting of the studied bivalves and regional oceanography of the Eastern Atlantic Ocean.

2 Material and methods

2.1 Material

Bivalve shells were selected from the collections belonging to the Muséum National d'Histoire Naturelle (MNHN) (Paris, France) (Table 1). We carefully chose pre-bomb specimens of known age and ensured that they were collected alive or very soon after death. For example, specimens with articulated valves, exhibiting flesh remains inside the shell were clearly collected alive. For *Senilia senilis*, the presence of the fragile periostracum provides evidence that the specimen was collected fresh. For *Bucardium ringens*, remains of the hinge ligament indicate that the bivalve death occurred not long before collection. The collection date was also carefully checked. Below, we provide background information for the five different bivalve species investigated in this study. Additional information for each sample is given in section 3.1.

Senilia senilis (Linnaeus, 1758) can be found from Mauritania to northern Angola. It lives in fine sand, estuaries, creeks or lagoons with regular tidal influence from the lower intertidal zone to about two metres water depth. This species tolerates seasonal salinity changes (von Cosel and Gofas, 2019). *S. senilis* is a suspension feeder that lives in the top 5-10-cm layer of sediment (Okera, 1976; Catry et al., 2017).

Bucardium ringens (Bruguière, 1789) is present from Mauritania to southern Angola. It lives in clean, fine sand and mixed sand on an open coast from shallow (5-10 metres depth) to about 50 metres depth. Shells and valves are commonly cast ashore on beaches but live-taken specimens are rare (von Cosel and Gofas, 2019). *B. ringens* is likely a suspension feeder as cardiids typically are (Herrera et al., 2015).

Donax rugosus (Linnaeus, 1758) is present from Mauritania to Ghana and from northern Angola to southern Angola. It lives in mixed, coarse sand in the surf zone of open beaches (von Cosel and Gofas, 2019). *D. rugosus* is a suspension feeder (Smith, 1971).

Ostrea stentina (Payraudeau, 1826) can be found from southern Portugal to Ghana, and from Gabon to northern Angola. It is common and occurs on various types of hard substrate such as rocks, stones, pebbles and other oysters from 1-to-30-metre depths. It can also be found in lagoons, inlets and creeks under marine conditions (von Cosel and Gofas, 2019). *O. stentina* is a suspension feeder (Türkmen et al., 2005).

Pseudochama gryphina (Lamarck, 1819) is present from southern Portugal to Mauritania and from Gabon to southern Angola (von Cosel and Gofas, 2019) and lives on hard substrate such as rocks and stones in clear water offshore in about 10 to 60 metres water depth. *P. gryphina* is a suspension feeder (Sessa et al., 2013).

A small piece (30-100 mg) of the outermost layers of each shell was cut using a Dremel™ rotary tool fitted with a cut-off wheel. We focused on the external part of the shell to ensure that we sampled and dated the most recent part (likely the last few months) of the specimen. The shell carbonate samples were then sonicated and rinsed in deionised water at least five times. Samples were coarsely crushed and split into a subsample for stable isotopic analysis and a subsample for ^{14}C analysis.

2.2 Radiocarbon measurements

Samples were washed with dilute HNO_3 (0.01M) for 15 mins then rinsed to neutral pH. Then, the shell carbonate was converted into CO_2 following LMC14 laboratory (Laboratoire de Mesure du Radiocarbone, Saclay, France) standard phosphoric acid hydrolysis procedure (Tisnérat-Laborde et al., 2001; Dumoulin et al., 2017). The CO_2 was then converted to graphite (Cottereau et al., 2007; Dumoulin et al., 2017) and analysed for its ^{14}C composition by Accelerator Mass Spectrometry (AMS) using the Artémis ^{14}C AMS facility (Moreau et al., 2013). Results are corrected for the $^{13}C/^{12}C$ ratio as measured on the AMS (Santos et al., 2007) and are reported in the $F^{14}C$ notation (Reimer et al., 2004). $F^{14}C$ is identical to the A_{SN}/A_{ON} metric (Stuiver and Polach, 1977), and the $^{14}a_N$ notation (Mook and van der Plicht, 1999). Corresponding conventional ^{14}C ages reported in ^{14}C years Before Present (AD 1950) were calculated according to:

$$^{14}C = -8033\ln(F^{14}C) \quad (3)$$

2.3 Stable carbon isotopes

Stable carbon and oxygen isotopic analyses of the dated samples were performed at the Pôle Spectrométrie Océan (PSO, Plouzané, France) using a MAT-253 (Thermo Scientific) stable isotope ratio mass spectrometer (IRMS) coupled with a Kiel IV Carbonate Device (Thermo Scientific). The measurements are reported versus Vienna Pee Dee Belemnite standard (VPDB) defined with respect to two international carbonate standards: NBS-19 ($\delta^{18}O$ = -2.20 ‰ and $\delta^{13}C$ = +1.95 ‰) and NBS-18 ($\delta^{18}O$ = -23.20 ‰ and $\delta^{13}C$ = -5.01 ‰). The mean external reproducibilities (1σ), based on repeated measurements of an in-house standard, were ±0.04‰ and ±0.02‰ for $\delta^{18}O$ and $\delta^{13}C$ values, respectively. Note that our samples integrate a seasonal variability of up 0.5 to 1‰ as shown by several investigations of growth layers in shells (e.g. Carré et al., 2005; Jones et al., 2007, 2010).

2.4 Marine Reservoir Age calculation

The marine reservoir age R of the selected shells is calculated according to equation (1) where t is the collection year as known from museum records (Table S1 in the Supplement and section results), $^{14}C_m$ is the measured shell ^{14}C age, and $^{14}C_{atm}$ is the ^{14}C age of the atmosphere. For shells picked from the northern hemisphere, $^{14}C_{atm}$ is obtained from the IntCal20 calibration curve (Reimer et al., 2020). For shells from the southern hemisphere, we used the southern hemisphere calibration curve SHCal20 (Hogg et al., 2020) instead. The uncertainty is calculated (Soulet, 2015) according to:

$$\sigma_{R(t)} = \sqrt{\sigma^2_{^{14}C_m(t)} + \sigma^2_{^{14}C_{atm}(t)}} \quad (4)$$

Note that mean SHCal20 offset compared to IntCal20 is estimated to be 36 ± 27 ^{14}C yrs. Thus, the R values calculated with IntCal20 or SHcal20 are essentially the same if one takes uncertainties into account.

The local marine reservoir offset ΔR of the selected shells is calculated according to equation (2) where t is the collection year as known from museum records (Table S1 in the Supplement and section results), $^{14}C_m$ is the measured shell ^{14}C age, and $^{14}C_{Marine20}$ is the ^{14}C age of the global marine calibration curve. Uncertainty is calculated as follows:

$$\sigma_{\Delta R(t)} = \sqrt{\sigma^2_{^{14}C_m(t)} + \sigma^2_{^{14}C_{Marine20}(t)}} \quad (5)$$

Note that Reimer and Reimer (2017) do not propagate the uncertainty of Marine20 calibration curve.

3 Results and Discussion

3.1 Radiocarbon measurement results

The detailed description of samples and results are shown in Table 1 and Table S1 in the Supplement. We classified the samples by location with corresponding geographic coordinates, then by species. Samples are coded as such “MNHN-IM-2022-xxxx” in order to locate the samples in the collections of the MNHN of Paris (France). The code “SacA-xxxxx” is the radiocarbon laboratory number.

3.2 West African marine reservoir ages

The vast majority of the calculated ΔR values, with a weighted mean value of -72 ± 42 ^{14}C yrs (1sd, n = 24), which corresponds to a weighted mean R value of 406 ± 56 ^{14}C yrs (1sd, n = 24), are typical of low latitude marine reservoir age values (Bard, 1988; Bard et al., 1994) (Table S1 in the Supplement, Fig. 1). Note that all averaged R and ΔR values were calculated according to the methodology recommended in the Marine Reservoir Correction Database (Reimer and Reimer, 2001; http://calib.org/marine/AverageDeltaR.html; last seen 31/05/2023). Our results agree perfectly with those already obtained (Ndeye, 2008) from the Nouadhibou-Cansado Bay area (Mauritania; Nh in Fig. 1) and Dakar area (Senegal; Dk in Fig. 1); the only two areas that we can compare our results with.

No significant interspecific differences were observed. This is best illustrated for the localities where reservoir age values were obtained from at least two different species for the same calendar time. In the Dakar area (Senegal; Dk in Fig. 1) for years 1908-1909 AD, we present data for five species (*Bucardium ringens*, *Donax rugosus*, *Mactra glabrata*, *Ostrea stentina*, *Senilia senilis*) (Ndeye, 2008; this study) all clustering within a range of [413;546] ([min; max]) with an average ΔR value of -18 ± 56 ^{14}C yrs (1sd, n = 6) (corresponding to an average R value of 465 ± 55 ^{14}C yrs). This was also the case for Luanda (Angola; Lu in Fig. 1) in the 1910 AD, with two species (*Donax rugosus* and *Senilia senilis*) yielding the same reservoir age values. This was further supported for the area of Nouadhibou-Cansado Bay (Mauritania) showing the same pattern (Ndeye, 2008; this study), although one sample out of four was likely an outlier (*Bucardium ringens* with # MNHN-IM-2022-4599). The fact that species living in very different ecological habitats (e.g. *Senilia senilis* in lagoons/semi-enclosed bays and *Donax rugosus* on beaches exposed to heavy surf; see also section material) show similar reservoir age values (R or ΔR) suggests that the habitat only exerts a minor influence on measured reservoir age in this region. The fact that all investigated species in this study correspond to suspension feeders further implies that suspension feeders are suitable material for reservoir age reconstruction.

Unlike semi-isolated basins such as the Baltic Sea (Lougheed et al., 2013) and Black Sea (Soulet et al., 2019), where the radiocarbon system is closely linked to the local oxygen/carbon stable isotopic system respectively, the open-ocean coastal region of West Africa is characterized by the lack of any relationship between reservoir age values (R or ΔR) and stable oxygen and carbon isotope compositions (r^2 of 0.02 and 0.001, respectively), as inferred from our results.

3.3 Marine reservoir evolution over time

Local marine reservoir ages were averaged over five-year windows ([1886- 1890 AD]-[1891-1895 AD] and so on), excluding the five outliers discussed in section 3.5. Sample with radiocarbon lab # AA-70015 (see Table S1 in the Supplement) is a single value from 1916 AD and was averaged with samples from year 1912 AD. We also calculated global marine reservoir age as the difference between the Marine20 and IntCal20 calibration curves. The evolution of the marine reservoir age of coastal West Africa (pink symbols in Fig. 2) shows a similar trend to that of the global marine reservoir age (black line in Fig. 2) with values declining steadily with time since ca. 1900 AD.

The ^{14}C age evolution of the global ocean (Marine20 calibration curve; Heaton et al., 2020) is constructed using the global carbon cycle model BICYCLE (Köhler et al., 2006; Köhler and Fischer, 2006, 2004; Köhler et al., 2005). This box model incorporates a globally averaged atmospheric box and modules of the terrestrial (seven boxes) and oceanic (10 boxes) components of the carbon cycle. It is driven by temporal changes in the boundary conditions mimicking changing climate and simulates changes in the carbon cycle including ^{14}C. To construct the Marine20 calibration curve, the BICYCLE model was revised to allow the atmospheric CO_2 and $F^{14}C$ to be specified externally (Heaton et al., 2020). While the modelled Marine20 (global surface ocean) radiocarbon age suggests constant values between 1900 and 1950 AD, our measured marine reservoir age R indicates instead a decreasing trend during that period, as a consequence of increasing atmospheric Intcal20 radiocarbon age. This observation of decreasing trend for R in West Africa between 1900 and 1950 AD could possibly reflect atmospheric $^{14}CO_2$ ageing following enhanced fossil fuel emissions to the atmosphere through burning (e.g. Suess, 1955; Tans et al., 1979)

3.4 Marine reservoir age off equatorial Ogooué and Congo rivers

Large rivers draining equatorial Africa such as the Ogooué and the Congo inject massive amounts of freshwater into the Atlantic Ocean (Lambert et al., 2015; Milliman and Farnsworth, 2011) leading to extensive sea surface salinity negative anomalies (Martins and Stammer, 2022). The sea surface salinity negative anomalies are associated with net primary productivity positive anomalies that are likely caused by the nutrient-rich river plumes from the Ogooué and Congo Rivers (Martins and Stammer, 2022). From a radiocarbon perspective, such net primary productivity positive anomalies should imply an increased uptake of atmospheric CO_2 through intensified biological pump. As a result, the reservoir age should be lower than average. The Congo River represents the second largest supplier of dissolved organic carbon (DOC) to the global ocean with ~5% of the land to ocean DOC flux (Spencer et al., 2016; Coynel et al., 2005; Richey et al., 2022). The DOC exported by the Congo river is ^{14}C-modern (Marwick et al., 2015; Spencer et al., 2012) and experiments showed that 45% of the Congo River DOC can potentially be photo-mineralised by sunlight (Spencer et al., 2009; Richey et al., 2022). Dissolved inorganic carbon (DIC) released from photo-mineralisation of the Congo River DOC should also be ^{14}C-modern. Thus, this modern DOC-derived DIC should impact the marine reservoir age towards values lower compared to average. There is a lack of available data to estimate the age and flux of dissolved CO_2 discharged by the Congo river into the ocean (Richey et al., 2022). Nevertheless, the marine reservoir age value measured at Port-Gentil (Gabon) close to the Ogooué river outlet is lower than the regional weighted mean value ($\Delta R = -106 \pm 63$ ^{14}C years, corresponding to $R = 329 \pm 21$ ^{14}C yrs) (PG in Fig. 1). The marine reservoir age measured in Pointe-Noire (Republic of Congo) ~150 km north of the Congo river outlet is also lower than the regional weighted mean value ($\Delta R = -156 \pm 64$ ^{14}C yrs; $R = 289 \pm 20$ ^{14}C yrs) (PN in Fig. 1). These values could be interpreted as having been influenced by Ogooué and Congo River discharges. However, all other localities close to the Congo River outlet had marine reservoir age close to the regional weighted mean value (Lo, Ca and Lu, in Fig. 1). Instead the lower values observed in Port-Gentil (Gabon) and Pointe-Noire (Republic of Congo) are from years 1948 and 1937 suggesting that these lower values are in line with the declining global marine reservoir evolution linked to the atmospheric CO_2 ^{14}C ageing linked to ^{14}C-dead input from fossil fuel burning (Suess effect) (see section 3.3). The impact of African equatorial rivers on the local/regional coastal marine reservoir age, if any, cannot be inferred from our results.

3.5 Outlier specimens

Mean marine reservoir age values (R and ΔR) are provided for West Africa based on our data, excluding five samples. These particular samples display much larger values with ΔR values ranging from 209 to 454 ^{14}C yrs or R values ranging from 701 to 912 ^{14}C yrs. Three specimens out of the five outlier samples correspond to *Bucardium ringens* specimens. We analysed 8 *Bucardium ringens* specimens. These three outlier specimens display reservoir age (R and ΔR) values that clearly disagree with neighbouring data (Nouadhibou-Cansado Bay, Loos Islands and Ivory Coast areas; Nh, LI and IC in Fig. 1). The Museum numbers of these specimens are MNHN-IM-2022-4597, MNHN-IM-2022-4599 and MNHN-IM-2022-4601. We do not expect that these larger values compared to those for neighbouring individuals come from the species feeding practice as they are all suspension feeders like all other investigated specimens. Similarly, we showed that the difference in the habitat in this region does not impact the species reservoir ages. Instead *Bucardium ringens* lives in the open coast from 5-10 metres to about 50 metres depth. Shells are commonly cast ashore on beaches but live-taken specimens are rare (von Cosel and Gofas, 2019). One of these outliers was collected at low tide (Roume Island in the Loos Islands; Republic of Guinea) and was devoid of flesh and hinge ligament. It is thus possible that this outlier sample was a transported subfossil sample that died a century or more before the collection date. The two other outlier samples had small remains of the hinge ligament (Nouadhibou; Mauritania and Jacqueville; Ivory Coast). It may be that these samples are also subfossil specimens. In this case, the hinge ligament must have been partially preserved owing to very favourable environmental conditions (Forman et al., 2004; Huntley et al., 2021). Alternatively, these outliers are not subfossil specimens and unlike the other species studied here, the habitat may exert an influence on R and ΔR values measured in *B. ringens*. Finally, we cannot fully rule out that these higher values represent some sub-annual variability of up to 200 ^{14}C in the local marine reservoir age as evidenced elsewhere (Jones et al., 2007, 2010). Nevertheless, five *Bucardium ringens* samples out of eight displayed reservoir age values in agreement with the neighbouring reservoir age values, this species might not be the best suited for reservoir age reconstruction or for sediment/archaeological dating.

The two remaining outliers are *Ostrea stentina* specimens from the El Jadida area (Morocco; eJ in Fig. 1). The sample from El Jadida beach was a single valve looking fresh and collected from the beach (museum # MNHN-IM-2022-4609). Based on the older ^{14}C age of this specimen, we cannot rule out that this sample could actually be a subfossil specimen. The specimen with museum code number # MNHN-IM-2022-4608 collected in the Sidi Moussa lagoon (south of El Jadida) was a specimen with articulated valves and remains of flesh inside the shell, meaning the specimen was still alive when collected. Variations in the reservoir age could be explained by coastal upwelling that impacts some regions of the Atlantic coast of Morocco and Western Sahara (Freudenthal et al., 2001; Barton et al., 1998). Upwelled waters are depleted in ^{14}C relative to the sea surface potentially causing larger reservoir age values (R or ΔR) like off Portugal (Monge Soares, 1993; Monge Soares and Alveirinho Dias, 2006), California (Kennett et al., 1997), Peru (Kennett et al., 2002; Fontugne et al., 2004; Jones et al., 2007, 2010) or Southern Arabian coast (Southon et al., 2002). Conversely, upwelled waters can also be nutrient-rich causing intensified ocean CO_2 uptake through enhanced primary production and biological pump (Williams and Follows, 2011), in which case, one could expect low-latitude average or decreased reservoir age values (R or ΔR). Off Morocco and the Western Sahara, the second hypothesis is most likely coastal upwelling which is known in this area to bring nutrient-rich waters to the surface ocean (Barton et al., 1998; Freudenthal et al., 2001), although to our knowledge no direct measurement of the ^{14}C content of coastal waters in this region has been published to date. However, according to recent studies, the El Jadida area is only weakly impacted by upwelling (Lourenço et al., 2020; Cropper et al., 2014), suggesting average reservoir age values instead of larger ones. Another explanation could be linked to the local hydrology of the Sidi Moussa lagoon. Despite the lagoon being permanently connected to the ocean, it receives waters from rainfall and resurgences that can have an impact on the salinity in the upstream section of the lagoon (Cheggour et al., 2001). As the surrounding rocks are calcareous sandstones (Manaan, 2003), one could hypothesise that freshwaters feeding the lagoon might be depleted in ^{14}C due to carbonate dissolution in the lagoon watershed causing a hardwater effect and thus a larger reservoir age. A last explanation could be an imperfect cleaning of the shell. For *Ostrea stentina*, sediment can be trapped between the growing layers of the shell. If this sediment contains old detrital carbonates, which were not perfectly removed before ^{14}C measurement, the ^{14}C age of the shell will appear older, and the reservoir age larger. Additional reservoir age reconstructions from this region on different species would be required to validate the larger reservoir age values reconstructed from the El Jadida area.

4 Conclusion

The analysis of pre-bomb suspension-feeding bivalves collected along coastal West Africa from 33°N to 15°S provides marine reservoir ages that are relatively homogenous, with a mean ΔR value of -72 ± 42 ^{14}C yrs (1sd, n = 24) and a mean R value of 406 ± 56 ^{14}C yrs (1sd, n = 24). When including the robust dataset from Ndeye (2008), the resulting mean ΔR and R values for coastal West Africa are -54 ± 51 ^{14}C years (1sd, n = 32) and 411 ± 61 ^{14}C years (1sd, n = 32), respectively. We show that the marine reservoir age of coastal West Africa is mainly driven by the global carbon cycle and atmospheric ^{14}C changes rather that by local effects.

Our results for different species yield similar marine reservoir age values, indicating that the ecological habitat only has a second-order impact on the reservoir age reconstruction, if any. Nevertheless, we suspect that *Bucardium ringens* might not be best suited for marine reservoir age reconstruction as corresponding shells are typically not found alive on sample collecting sites. Additionally, ages obtained on *Ostrea stentina* could be possibly influenced by the presence of sediment within the growing shell layers if not fully removed after the cleaning process.

Despite these new data, large portions of the West African coast still remain to be investigated for reservoir age reconstructions, in particular off Western Sahara and Canarias Islands, Sierra Leone-Liberia, Nigeria and Namibia.

Author contribution statement

GSoulet designed the study and raised the funding. SG, PM, GSoulet and GSiani selected the specimens in the MNHN collections. GSoulet carried out the sample preparation with assistance of ML and FF. FD performed stable isotopes measurements. GSoulet performed reservoir calculations and analysed and discussed the data with GB, GSiani and SG. GSoulet wrote the manuscript with inputs from all co-authors.

Acknowledgements

All authors thank Michel Fontugne, an anonymous reviewer and Paula Reimer for reviewing the manuscript. We are grateful to the Muséum National d'Histoire Naturelle (Paris, France) for providing the samples. We thank the LMC14 staff (Laboratoire de Mesure du Carbone-14) and the CNRS-INSU ARTEMIS national radiocarbon AMS facility for providing radiocarbon measurements published in this study. The study was funded by the French national program INSU-LEFE (ResWA project – Pre-bomb Reservoir ages for the Western coast of Africa). We are grateful to Alison Chalm (Ifremer, Brest) for English editing. I (GS) thank Ifremer in Brest and Sète for supporting my research. Finally, this study was carried out and the paper written during my part-time parental leave. I dedicate this article to Marian, with whom I have had a wonderful time during this year, growing up together, him as a toddler and me as a father.

Competing interests

The authors declare that they have no conflict of interest.

Data availability

All data present in the paper are available in the text section 3.1 and in Table S1 in the Supplement.

References

Alves, E. Q., Macario, K., Ascough, P., and Bronk Ramsey, C.: The worldwide marine radiocarbon reservoir effect: Definitions, mechanisms, and prospects, Rev. Geophys., 56, 278–305, https://doi.org/10.1002/2017RG000588, 2018.

Alves, E. Q., Macario, K. D., Urrutia, F. P., Cardoso, R. P., and Bronk Ramsey, C.: Accounting for the marine reservoir effect in radiocarbon calibration, Quat. Sci. Rev., 209, 129–138, https://doi.org/10.1016/j.quascirev.2019.02.013, 2019.

Arnold, J. R. and Anderson, E. C.: The distribution of Carbon-14 in nature, Tellus, 9, 28–32, https://doi.org/10.1111/j.2153-3490.1957.tb01850.x, 1957.

Ascough, P., Cook, G., and Dugmore, A.: Methodological approaches to determining the marine radiocarbon reservoir effect, Prog. Phys. Geogr. Earth Environ., 29, 532–547, https://doi.org/10.1191/0309133305pp461ra, 2005.

Bard, E.: Correction of accelerator mass spectrometry ^{14}C ages measured in planktonic foraminifera: Paleoceanographic implications, Paleoceanography, 3, 635–645, https://doi.org/10.1029/PA003i006p00635, 1988.

Bard, E., Arnold, M., Mangerud, J., Paterne, M., Labeyrie, L., Duprat, J., Mélières, M.-A., Sønstegaard, E., and Duplessy, J.-C.: The North Atlantic atmosphere-sea surface ^{14}C gradient during the Younger Dryas climatic event, Earth Planet. Sci. Lett., 126, 275–287, https://doi.org/10.1016/0012-821X(94)90112-0, 1994.

Barton, E. D., Arístegui, J., Tett, P., Cantón, M., García-Braun, J., Hernández-León, S., Nykjaer, L., Almeida, C., Almunia, J., Ballesteros, S., Basterretxea, G., Escánez, J., García-Weill, L., Hernández-Guerra, A., López-Laatzen, F., Molina, R., Montero, M. F., Navarro-Pérez, E., Rodríguez, J. M., van Lenning, K., Vélez, H., and Wild, K.: The transition zone of the Canary Current upwelling region, Prog. Oceanogr., 41, 455–504, https://doi.org/10.1016/S0079-6611(98)00023-8, 1998.

Boettger, C. R.: Zur Molluskenfauna des Kongogebiets, Ann. la Société R. Zool. Malacol. Belgique, 47, 89–117, 1912.

Boettger, O.: Katalog der Reptilien-Sammlung im Museum der Senckenbergischen Naturforschenden Gesellschaft in Frankfurt am Main, II Teil (Schlangen), Gebrüder Knauer, Frankfurt am Main, 1898.

Butzin, M., Köhler, P., and Lohmann, G.: Marine radiocarbon reservoir age simulations for the past 50,000 years, Geophys. Res. Lett., 44, 8473–8480, https://doi.org/10.1002/2017GL074688, 2017.

Carré, M., Bentaleb, I., Blamart, D., Ogle, N., Cardenas, F., Zevallos, S., Kalin, R. M., Ortlieb, L., and Fontugne, M.: Stable isotopes and sclerochronology of the bivalve Mesodesma donacium: Potential application to Peruvian paleoceanographic reconstructions, Palaeogeogr. Palaeoclimatol. Palaeoecol., 228, 4–25, https://doi.org/10.1016/j.palaeo.2005.03.045, 2005.

Catry, T., Figueira, P., Carvalho, L., Monteiro, R., Coelho, P., Lourenço, P. M., Catry, P., Tchantchalam, Q., Catry, I., Botelho, M. J., Pereira, E., Granadeiro, J. P., and Vale, C.: Evidence for contrasting accumulation pattern of cadmium in relation to other elements in Senilia senilis and Tagelus adansoni from the Bijagós archipelago, Guinea-Bissau, Environ. Sci. Pollut. Res., 24, 24896–24906, https://doi.org/10.1007/s11356-017-9902-8, 2017.

Cheggour, M., Chafik, A., Langston, W. ., Burt, G. ., Benbrahim, S., and Texier, H.: Metals in sediments and the edible cockle Cerastoderma edule from two Moroccan Atlantic lagoons: Moulay Bou Selham and Sidi Moussa, Environ. Pollut., 115, 149–160, https://doi.org/10.1016/S0269-7491(01)00117-8, 2001.

von Cosel, R. and Gofas, S.: Marine Bivalves of Tropical West Africa: From Rio de Oro to Southern Angola, edited by: MNHN and IRD, Faune et Flore tropicales, 48, Paris, Marseille, 1104 pp., 2019.

Cottereau, E., Arnold, M., Moreau, C., Baqué, D., Bavay, D., Caffy, I., Comby, C., Dumoulin, J.-P., Hain, S., Perron, M., Salomon, J., and Setti, V.: Artemis, the new ^{14}C AMS at LMC14 in Saclay, France, Radiocarbon, 49, 291–299, https://doi.org/10.1017/S0033822200042211, 2007.

Coynel, A., Seyler, P., Etcheber, H., Meybeck, M., and Orange, D.: Spatial and seasonal dynamics of total suspended sediment and organic carbon species in the Congo River, Global Biogeochem. Cycles, 19, n/a-n/a, https://doi.org/10.1029/2004GB002335, 2005.

Craig, H.: The natural distribution of radiocarbon and the exchange time of carbon dioxide between atmosphere and sea, Tellus, 9, 1–17, https://doi.org/10.1111/j.2153-3490.1957.tb01848.x, 1957.

Cropper, T. E., Hanna, E., and Bigg, G. R.: Spatial and temporal seasonal trends in coastal upwelling off Northwest Africa, 1981–2012, Deep Sea Res. Part I Oceanogr. Res. Pap., 86, 94–111, https://doi.org/10.1016/j.dsr.2014.01.007, 2014.

Dautzenberg, P.: Mission Gruvel sur la côte occidentale d'Afrique (1909-1910): Mollusques marins. Annales de l'Institut Océanographique, Paris (Nouvelle Série). 5(3): 1-111, pl. 1-3, 1912.

Dewar, G., Reimer, P. J., Sealy, J., and Woodborne, S.: Late-Holocene marine radiocarbon reservoir correction (ΔR) for the west coast of South Africa, The Holocene, 22, 1481–1489, https://doi.org/10.1177/0959683612449755, 2012.

Dumoulin, J.-P., Comby-Zerbino, C., Delqué-Količ, E., Moreau, C., Caffy, I., Hain, S., Perron, M., Thellier, B., Setti, V., Berthier, B., and Beck, L.: Status report on sample preparation protocols developed at the LMC14 laboratory, Saclay, France: From Sample Collection to ^{14}C AMS Measurement, Radiocarbon, 59, 713–726, https://doi.org/10.1017/RDC.2016.116, 2017.

Fontugne, M., Carré, M., Bentaleb, I., Julien, M., and Lavallée, D.: Radiocarbon reservoir age variations in the south Peruvian upwelling during the Holocene, Radiocarbon, 46, 531–537, https://doi.org/10.1017/S003382220003558X, 2004.

Forman, S.: A review of postglacial emergence on Svalbard, Franz Josef Land and Novaya Zemlya, northern Eurasia, Quat. Sci. Rev., 23, 1391–1434, https://doi.org/10.1016/j.quascirev.2003.12.007, 2004.

Freudenthal, T., Neuer, S., Meggers, H., Davenport, R., and Wefer, G.: Influence of lateral particle advection and organic matter degradation on sediment accumulation and stable nitrogen isotope ratios along a productivity gradient in the Canary Islands region, Mar. Geol., 177, 93–109, https://doi.org/10.1016/S0025-3227(01)00126-8, 2001.

Heaton, T. J., Köhler, P., Butzin, M., Bard, E., Reimer, R. W., Austin, W. E. N., Bronk Ramsey, C., Grootes, P. M., Hughen, K. A., Kromer, B., Reimer, P. J., Adkins, J., Burke, A., Cook, M. S., Olsen, J., and Skinner, L. C.: Marine20—The Marine Radiocarbon Age Calibration Curve (0–55,000 cal BP), Radiocarbon, 62, 779–820, https://doi.org/10.1017/RDC.2020.68, 2020.

Heaton, T. J., Bard, E., Bronk Ramsey, C., Butzin, M., Köhler, P., Muscheler, R., Reimer, P. J., and Wacker, L.: Radiocarbon: A key tracer for studying Earth's dynamo, climate system, carbon cycle, and Sun, Science (80-.)., 374, https://doi.org/10.1126/science.abd7096, 2021.

Heaton, T. J., Bard, E., Bronk Ramsey, C., Butzin, M., Hatté, C., Hughen, K. A., Köhler, P., and Reimer, P. J.: A response to community questions on the Marine20 radiocarbon age calibration curve: Marine reservoir ages and the calibration of ^{14}C samples from the oceans, Radiocarbon, 65, 247–273, https://doi.org/10.1017/RDC.2022.66, 2023.

Herrera, N. D., ter Poorten, J. J., Bieler, R., Mikkelsen, P. M., Strong, E. E., Jablonski, D., and Steppan, S. J.: Molecular phylogenetics and historical biogeography amid shifting continents in the cockles and giant clams (Bivalvia: Cardiidae), Mol. Phylogenet. Evol., 93, 94–106, https://doi.org/10.1016/j.ympev.2015.07.013, 2015.

Hogg, A. G., Heaton, T. J., Hua, Q., Palmer, J. G., Turney, C. S., Southon, J., Bayliss, A., Blackwell, P. G., Boswijk, G., Bronk Ramsey, C., Pearson, C., Petchey, F., Reimer, P., Reimer, R., and Wacker, L.: SHCal20 Southern Hemisphere Calibration, 0–55,000 Years cal BP, Radiocarbon, 62, 759–778, https://doi.org/10.1017/RDC.2020.59, 2020.

Huntley, J. W., De Baets, K., Scarponi, D., Linehan, L. C., Epa, Y. R., Jacobs, G. S., and Todd, J. A.: Bivalve mollusks as hosts in the fossil record, in: The Evolution and Fossil Record of Parasitism, edited by: De Baets, K. and Huntley, J. W., Springer International Publishing, 251–287, https://doi.org/10.1007/978-3-030-52233-9_8, 2021.

Kennett, D. J., Ingram, B. L., Erlandson, J. M., and Walker, P.: Evidence for Temporal Fluctuations in Marine Radiocarbon Reservoir Ages in the Santa Barbara Channel, Southern California, J. Archaeol. Sci., 24, 1051–1059, https://doi.org/10.1006/jasc.1996.0184, 1997.

Kennett, D. J., Lynn Ingram, B., Southon, J. R., and Wise, K.: Differences in ^{14}C age between stratigraphically associated charcoal and marine shell from the Archaic Period Site of Kilometer 4, Southern Peru: Old wood or old water?, Radiocarbon, 44, 53–58, https://doi.org/10.1017/S0033822200064663, 2002.

Köhler, P. and Fischer, H.: Simulating changes in the terrestrial biosphere during the last glacial/interglacial transition, Glob. Planet. Change, 43, 33–55, https://doi.org/10.1016/j.gloplacha.2004.02.005, 2004.

Köhler, P. and Fischer, H.: Simulating low frequency changes in atmospheric CO_2 during the last 740 000 years, Clim. Past, 2, 57–78, https://doi.org/10.5194/cp-2-57-2006, 2006.

Köhler, P., Fischer, H., Munhoven, G., and Zeebe, R. E.: Quantitative interpretation of atmospheric carbon records over the last glacial termination, Global Biogeochem. Cycles, 19, n/a-n/a, https://doi.org/10.1029/2004GB002345, 2005.

Köhler, P., Muscheler, R., and Fischer, H.: A model-based interpretation of low-frequency changes in the carbon cycle during the last 120,000 years and its implications for the reconstruction of atmospheric $\Delta^{14}C$, Geochemistry, Geophys. Geosystems, 7, n/a-n/a, https://doi.org/10.1029/2005GC001228, 2006.

Lambert, T., Darchambeau, F., Bouillon, S., Alhou, B., Mbega, J.-D., Teodoru, C. R., Nyoni, F. C., Massicotte, P., and Borges, A. V.: Landscape control on the spatial and temporal variability of chromophoric dissolved organic matter and dissolved organic carbon in large African Rivers, Ecosystems, 18, 1224–1239, https://doi.org/10.1007/s10021-015-9894-5, 2015.

Lindsay, C. M., Lehman, S. J., Marchitto, T. M., Carriquiry, J. D., and Ortiz, J. D.: New constraints on deglacial marine radiocarbon anomalies from a depth transect near Baja California, Paleoceanography, 31, 1103–1116, https://doi.org/10.1002/2015PA002878, 2016.

Lougheed, B. C., Filipsson, H. L., and Snowball, I.: Large spatial variations in coastal ^{14}C reservoir age – a case study from the Baltic Sea, Clim. Past, 9, 1015–1028, https://doi.org/10.5194/cp-9-1015-2013, 2013.

Lourenço, C. R., Nicastro, K. R., McQuaid, C. D., Krug, L. A., and Zardi, G. I.: Strong upwelling conditions drive differences in species abundance and community composition along the Atlantic coasts of Morocco and Western Sahara, Mar. Biodivers., 50, 15, https://doi.org/10.1007/s12526-019-01032-z, 2020.

Manaan, M.: Étude sédimentologique du remplissage de la lagune de Sidi Moussa, Maroc, PhD thesis, Université Chouaib Doukkali, El Jadida, https://theses.hal.science/tel-00124571, 2003.

Martins, M. S. and Stammer, D.: Interannual variability of the Congo River plume-induced sea surface salinity, Remote Sens., 14, 1013, https://doi.org/10.3390/rs14041013, 2022.

Marwick, T. R., Tamooh, F., Teodoru, C. R., Borges, A. V., Darchambeau, F., and Bouillon, S.: The age of river-transported carbon: A global perspective, Global Biogeochem. Cycles, 29, 122–137, https://doi.org/10.1002/2014GB004911, 2015.

Milliman, J. D. and Farnsworth, K. L.: River discharge to the coastal ocean, Cambridge University Press, https://doi.org/10.1017/CBO9780511781247, 2011.

Monge Soares, A.: The ^{14}C content of marine shells: Evidence for variability in coastal upwelling off Portugal during the Holocene, in: Isotope techniques in the study of past and current environmental changes in the hydrosphere and the atmosphere proceedings, edited by: IAEA, Vienna, 471–485, 1993.

Monge Soares, A. M. and Alveirinho Dias, J. M.: Coastal upwelling and radiocarbon-evidence for temporal fluctuations in ocean reservoir effect off portugal during the holocene, Radiocarbon, 48, 45–60, https://doi.org/10.1017/S0033822200035384, 2006.

Mook, W. G. and van der Plicht, J.: Reporting ^{14}C activities and concentrations, Radiocarbon, 41, 227–239, https://doi.org/10.1017/S0033822200057106, 1999.

Moreau, C., Caffy, I., Comby, C., Delqué-Količ, E., Dumoulin, J.-P., Hain, S., Quiles, A., Setti, V., Souprayen, C., Thellier, B., and Vincent, J.: Research and development of the Artemis ^{14}C AMS facility: Status report, Radiocarbon, 55, 331–337, https://doi.org/10.1017/S0033822200057441, 2013.

Ndeye, M.: Marine reservoir ages in Northern Senegal and Mauritania coastal waters, Radiocarbon, 50, 281–288, https://doi.org/10.1017/S0033822200033580, 2008.

Okera, W.: Observations on some population parameters of exploited stocks of Senilia senilis (=Arca senilis) in Sierra Leone, Mar. Biol., 38, 217–229, https://doi.org/10.1007/BF00388935, 1976.

Oliver, P. G. and von Cosel, R.: Taxonomy of tropical west African Bivalves. IV. Arcidae., Bull. Muséum Natl. d'Histoire Nat., 14, 293–381, 1992.

Reimer, P. J. and McCormac, F. G.: Marine radiocarbon reservoir corrections for the Mediterranean and Aegean Seas, Radiocarbon, 44, 159–166, https://doi.org/10.1017/S0033822200064766, 2002.

Reimer, P. J. and Reimer, R. W.: A marine reservoir correction database and on-line interface, Radiocarbon, 43, 461–463, https://doi.org/10.1017/S0033822200038339, 2001.

Reimer, P. J., Brown, T. A., and Reimer, R. W.: Discussion: Reporting and calibration of post-bomb ^{14}C data, Radiocarbon, 46, 1299–1304, https://doi.org/10.1017/S0033822200033154, 2004.

Reimer, P. J., Austin, W. E. N., Bard, E., Bayliss, A., Blackwell, P. G., Bronk Ramsey, C., Butzin, M., Cheng, H., Edwards, R. L., Friedrich, M., Grootes, P. M., Guilderson, T. P., Hajdas, I., Heaton, T. J., Hogg, A. G., Hughen, K. A., Kromer, B., Manning, S. W., Muscheler, R., Palmer, J. G., Pearson, C., van der Plicht, J., Reimer, R. W., Richards, D. A., Scott, E. M., Southon, J. R., Turney, C. S. M., Wacker, L., Adolphi, F., Büntgen, U., Capano, M., Fahrni, S. M., Fogtmann-Schulz, A., Friedrich, R., Köhler, P., Kudsk, S., Miyake, F., Olsen, J., Reinig, F., Sakamoto, M., Sookdeo, A., and Talamo, S.: The IntCal20 northern hemisphere radiocarbon age calibration curve (0–55 cal kBP), Radiocarbon, 62, 725–757, https://doi.org/10.1017/RDC.2020.41, 2020.

Reimer, R. W. and Reimer, P. J.: An online application for ΔR calculation, Radiocarbon, 59, 1623–1627, https://doi.org/10.1017/RDC.2016.117, 2017.

Revelle, R. and Suess, H. E.: Carbon dioxide exchange between atmosphere and ocean and the question of an increase of atmospheric CO_2 during the past decades, Tellus, 9, 18–27, https://doi.org/10.1111/j.2153-3490.1957.tb01849.x, 1957.

Richey, J. E., Spencer, R. G. M., Drake, T. W., and Ward, N. D.: Fluvial carbon dynamics across the land to ocean continuum of great tropical rivers, 391–412, https://doi.org/10.1002/9781119657002.ch20, 2022.

Roux, C.: Compte rendu sommaire d'une mission en Afrique Équatoriale Française, Bull. du Muséum Natl. d'Histoire Nat., 21, 500–503, 1949.

Santos, G. M., Southon, J. R., Griffin, S., Beaupre, S. R., and Druffel, E. R. M.: Ultra small-mass AMS ^{14}C sample preparation and analyses at KCCAMS/UCI Facility, Nucl. Instruments Methods Phys. Res. Sect. B Beam Interact. with Mater. Atoms, 259, 293–302, https://doi.org/10.1016/j.nimb.2007.01.172, 2007.

Schefuß, E., Eglinton, T. I., Spencer-Jones, C. L., Rullkötter, J., De Pol-Holz, R., Talbot, H. M., Grootes, P. M., and Schneider, R. R.: Hydrologic control of carbon cycling and aged carbon discharge in the Congo River basin, Nat. Geosci., 9, 687–690, https://doi.org/10.1038/ngeo2778, 2016.

Sessa, J. A., Callapez, P. M., Dinis, P. A., and Hendy, A. J. W.: Paleoenvironmental and paleobiogeographical implications of a middle Pleistocene mollusc assemblage from the marine terraces of Baía Das Pipas, southwest Angola, J. Paleontol., 87, 1016–1040, https://doi.org/10.1666/12-119, 2013.

Siani, G., Paterne, M., Arnold, M., Bard, E., Métivier, B., Tisnerat, N., and Bassinot, F.: Radiocarbon reservoir ages in the Mediterranean Sea and Black Sea, Radiocarbon, 42, 271–280, https://doi.org/10.1017/S0033822200059075, 2000.

Siani, G., Paterne, M., Michel, E., Sulpizio, R., Sbrana, A., Arnold, M., and Haddad, G.: Mediterranean Sea surface radiocarbon reservoir age changes since the Last Glacial Maximum, Science (80-.)., 294, 1917–1920, https://doi.org/10.1126/science.1063649, 2001.

Siegenthaler, U.: Uptake of excess CO_2 by an outcrop-diffusion model of the ocean, J. Geophys. Res., 88, 3599, https://doi.org/10.1029/JC088iC06p03599, 1983.

Skinner, L., McCave, I. N., Carter, L., Fallon, S., Scrivner, A. E., and Primeau, F.: Reduced ventilation and enhanced magnitude of the deep Pacific carbon pool during the last glacial period, Earth Planet. Sci. Lett., 411, 45–52, https://doi.org/10.1016/j.epsl.2014.11.024, 2015.

Skinner, L. C. and Bard, E.: Radiocarbon as a dating tool and tracer in paleoceanography, Rev. Geophys., 60, 1–64, https://doi.org/10.1029/2020RG000720, 2022.

Skinner, L. C., Fallon, S., Waelbroeck, C., Michel, E., and Barker, S.: Ventilation of the deep Southern Ocean and deglacial CO_2 rise, Science (80-.)., 328, 1147–1151, https://doi.org/10.1126/science.1183627, 2010.

Smith, D. A. S.: Polymorphism and population density in Donax rugosus (Lamellibranchiata: Donacidae), J. Zool., 164, 429–441, https://doi.org/10.1111/j.1469-7998.1971.tb01327.x, 1971.

Soulet, G.: Methods and codes for reservoir–atmosphere ^{14}C age offset calculations, Quat. Geochronol., 29, 97–103, https://doi.org/10.1016/j.quageo.2015.05.023, 2015.

Soulet, G., Ménot, G., Garreta, V., Rostek, F., Zaragosi, S., Lericolais, G., and Bard, E.: Black Sea “Lake” reservoir age evolution since the Last Glacial — Hydrologic and climatic implications, Earth Planet. Sci. Lett., 308, 245–258, https://doi.org/10.1016/j.epsl.2011.06.002, 2011.

Soulet, G., Skinner, L. C., Beaupré, S. R., and Galy, V.: A note on reporting of reservoir ^{14}C disequilibria and age offsets, Radiocarbon, 58, 205–211, https://doi.org/10.1017/RDC.2015.22, 2016.

Soulet, G., Giosan, L., Flaux, C., and Galy, V.: Using stable carbon isotopes to quantify radiocarbon reservoir age offsets in the coastal black sea, Radiocarbon, 61, https://doi.org/10.1017/RDC.2018.61, 2019.

Southon, J., Kashgarian, M., Fontugne, M., Metivier, B., and Yim, W. W. S.: Marine reservoir corrections for the Indian Ocean and Southeast Asia, Radiocarbon, 44, 167–180, https://doi.org/10.1017/S0033822200064778, 2002.

Spencer, R. G. M., Stubbins, A., Hernes, P. J., Baker, A., Mopper, K., Aufdenkampe, A. K., Dyda, R. Y., Mwamba, V. L., Mangangu, A. M., Wabakanghanzi, J. N., and Six, J.: Photochemical degradation of dissolved organic matter and dissolved lignin phenols from the Congo River, J. Geophys. Res., 114, G03010, https://doi.org/10.1029/2009JG000968, 2009.

Spencer, R. G. M., Hernes, P. J., Aufdenkampe, A. K., Baker, A., Gulliver, P., Stubbins, A., Aiken, G. R., Dyda, R. Y., Butler, K. D., Mwamba, V. L., Mangangu, A. M., Wabakanghanzi, J. N., and Six, J.: An initial investigation into the organic matter biogeochemistry of the Congo River, Geochim. Cosmochim. Acta, 84, 614–627, https://doi.org/10.1016/j.gca.2012.01.013, 2012.

Spencer, R. G. M., Hernes, P. J., Dinga, B., Wabakanghanzi, J. N., Drake, T. W., and Six, J.: Origins, seasonality, and fluxes of organic matter in the Congo River, Global Biogeochem. Cycles, 30, 1105–1121, https://doi.org/10.1002/2016GB005427, 2016.

Stuiver, M. and Braziunas, T. F.: Modeling atmospheric ^{14}C influences and ^{14}C ages of marine samples to 10,000 BC, Radiocarbon, 35, 137–189, https://doi.org/10.1017/S0033822200013874, 1993.

Stuiver, M. and Polach, H. A.: Discussion: Reporting of ^{14}C Data, Radiocarbon, 19, 355–363, https://doi.org/10.1017/S0033822200003672, 1977.

Stuiver, M., Pearson, G. W., and Braziunas, T.: Radiocarbon age calibration of marine samples back to 9000 cal yr BP, Radiocarbon, 28, 980–1021, https://doi.org/10.1017/S0033822200060264, 1986.

Suess, H. E.: Radiocarbon concentration in modern wood, Science, 122, 415–417, https://doi.org/10.1126/science.122.3166.415.b, 1955.

Tans, P. P., De Jong, A. F. M., and Mook, W. G.: Natural atmospheric ^{14}C variation and the Suess effect, Nature, 280, 826–828, https://doi.org/10.1038/280826a0, 1979.

Tisnérat-Laborde, N., Poupeau, J. J., Tannau, J. F., and Paterne, M.: Development of a semi-automated system for routine preparation of carbonate samples, Radiocarbon, 43, 299–304, https://doi.org/10.1017/S0033822200038145, 2001.

Türkmen, A., Türkmen, M., and Tepe, Y.: Biomonitoring of heavy metals from Iskenderun Bay using two bivalve species Chama pacifica Broderip, 1834 and Ostrea stentina Payraudeau, 1826, Turkish J. Fish. Aquat. Sci., 5, 107–111, 2005.

Westhoff, F.: Die Fauna der Kongo-Mündung, Jahresbericht der Zool. Sekt. Westfälischen Prov. Vereins für Wiss. und Kunſt für das Etatsjahr 1885-86, 38–40, 1886.

Williams, R. G. and Follows, M. J.: Ocean dynamics and the carbon cycle: Principles and mechanisms, Cambridge., Cambridge, 434 pp., 2011.

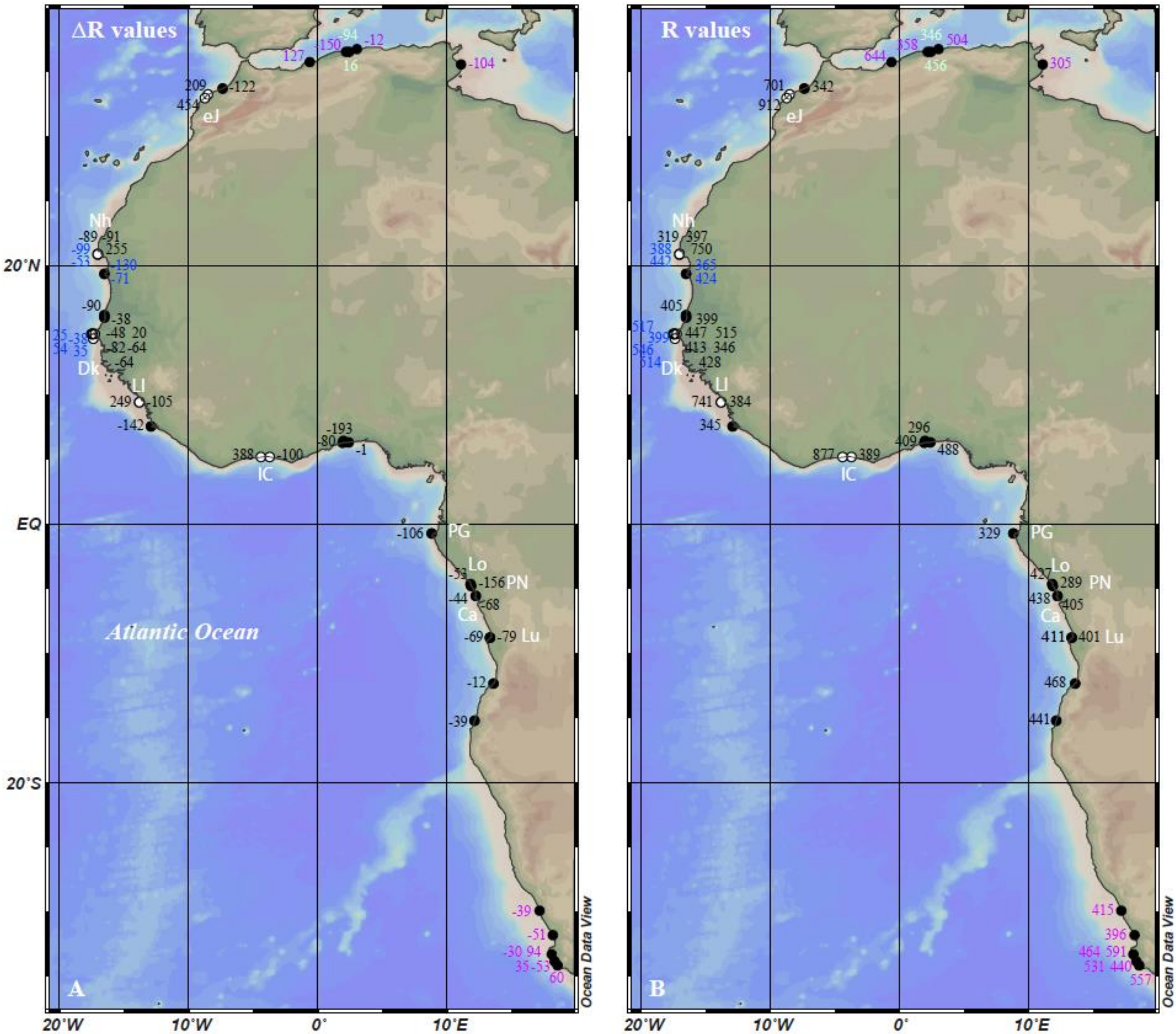

Figure 1: The geographic distribution of marine reservoir age values along the West African coast. A. ΔR values. B. R values. Data shown in black are from this study. Others are selected results from previous studies discussed in the text, converted from their original format (conventional 14C ages and collection dates) to ΔR and R values using the latest calibration curves Marine20 (Heaton et al., 2020) and Intcal20 or SHcal20 (Reimer et al., 2020; Hogg et al., 2020), respectively. Data in blue are from Ndeye (2008), data in green are from (Reimer and McCormac, 2002), data in purple are from (Siani et al., 2000) and data in pink are from (Dewar et al., 2012). eJ, Nh, Dk, LI, IC, PG, Lo, PN, Ca and Lu stand for el Jadida (Morocco), Nouadhibou (Mauritania), Dakar (Senegal), Loos Islands (Republic of Guinea), Ivory Coast, Port-Gentil (Gabon), Loango (Republic of Congo), Pointe Noire (Republic of Congo), Cabinda (Angola) and Luanda (Angola). The map was drawn using Ocean Data View (Schlitzer, Reiner, Ocean Data View, https://odv.awi.de, 2022).

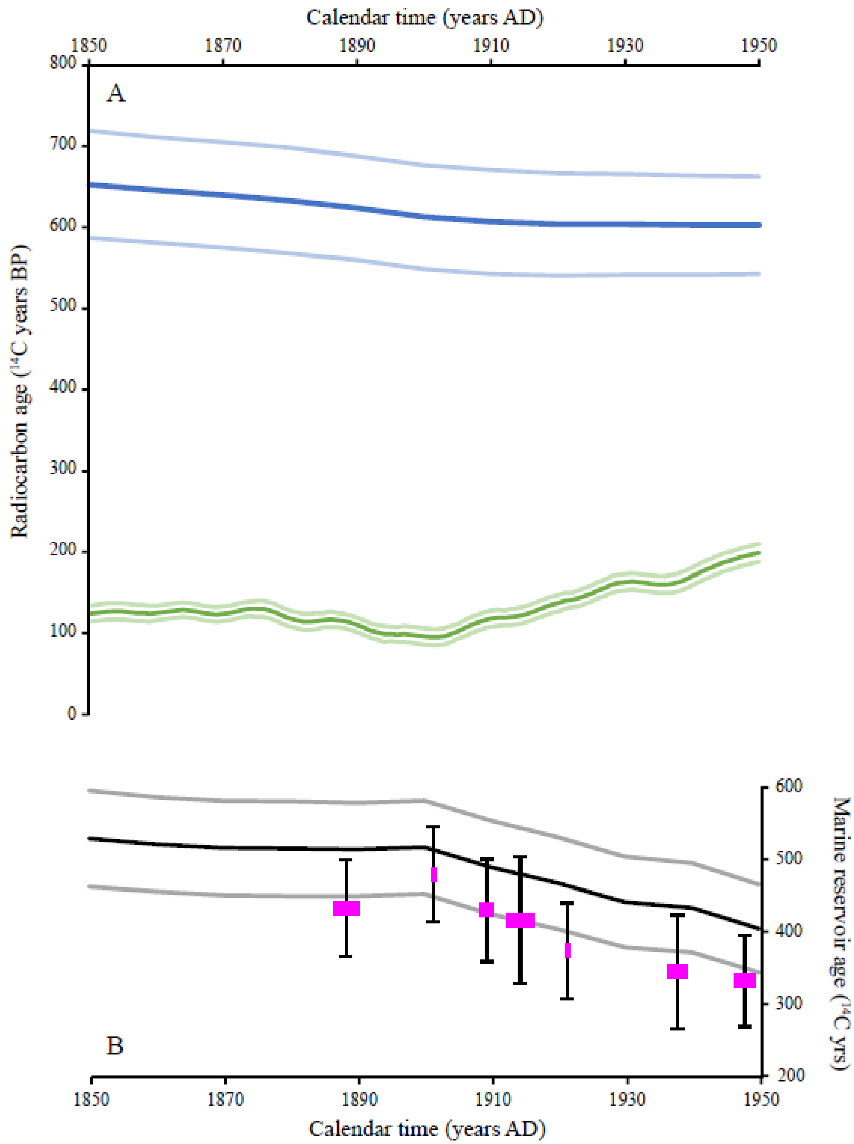

Figure 2: A: The radiocarbon-age evolution of the atmosphere (IntCal20; green curve with its light green 1-σ envelope) and of the global ocean (Marine20; blue curve with its light blue 1-σ envelope) between 1850 and 1950 AD. B: The global marine reservoir age (black curve with its grey 1-σ envelope) calculated as the difference between Marine20 and Intcal20 curves. Pink symbols are the coastal West African marine reservoir age calculated by averaging data over 5-yr windows. The reported error bars are the maximum of the standard deviation of the averaged data and the individual uncertainty of the averaged data.

Table 1: Description of the samples and results

Museum ID	Species	Location	Sample description	Lab ID $F^{14}C$ and ^{14}C age BP) ^{13}C (‰ VPDB)	Year (AD)	Collector	Museum label and note
Morocco							
MNHN-IM-2022-4615	*Ostrea stentina*	Mohammedia (33.71°N, 7.37°W)	Articulated specimen with remains of flesh	SacA-68834 $F^{14}C = 0.9418 \pm 0.0021$ (482 ± 18 BP) $\delta^{13}C = 1.19$ ‰ VPDB	1921	Jacques de Lépiney	Ostrea stentina Payr, Fedhala 1921, donat J de Lépiney 1939
MNHN-IM-2022-4609	*Ostrea stentina*	El Jadida, beach (33.25°N, 8.49°W)	An isolated valve looking quite fresh	SacA-68828 $F^{14}C = 0.9033 \pm 0.0020$ (817 ± 18 BP) $\delta^{13}C = 0.71$ ‰ VPDB	October 26th 1909	Louis Gentil	Plage de Mazagan 26 octobre 1909, Maroc, Louis Gentil
MNHN-IM-2022-4608	*Ostrea stentina*	Lagoon of Sidi Moussa (32.98°N, 8.75°W)	Articulated specimen with remains of flesh.	SacA-68827 $F^{14}C = 0.8766 \pm 0.0021$ (1058 ± 19 BP) $\delta^{13}C = -0.48$ ‰ VPDB	1924	Jacques de Lépiney	Ostrea stentina Payr., lagune de Sidi Moussa (région de Mazagan), 1924, donat. J de Lépiney 1939
Mauritania							
MNHN-IM-2022-4612	*Ostrea stentina*	Nouadhibou, Pointe Chacal (20.91°N, 17.04°W)	Articulated specimen.	SacA-68831 $F^{14}C = 0.9381 \pm 0.0020$ (514 ± 17 BP) $\delta^{13}C = 2.28$ ‰ VPDB	1948	Roger Sourie	Port Etienne (Pointe des Chacals) M. Sourie, 1948
MNHN-IM-2022-4610	*Ostrea stentina*	Cansado Bay (20.88°N, 17.04°W)	Articulated specimen with remains of flesh.	SacA-68829 $F^{14}C = 0.9378 \pm 0.0020$ (516 ± 17 BP) $\delta^{13}C = 2.09$ ‰ VPDB	1911-1912	Mission Gruvel	Ostrea stentina Payr. = lacerans Hanl., Baie de Cansado, Mission Gruvel, 1911-1912
MNHN-IM-2022-4599	*Bucardium ringens*	Nouadhibou (20.88°N, 17.04°W)	An isolated valve of a juvenile with remains of the hinge ligament.	SacA-68811 $F^{14}C = 0.8981 \pm 0.0020$ (863 ± 18 BP) $\delta^{13}C = 0.38$ ‰ VPDB	1908	Mission Gruvel	Cardium ringens Gmelin; Port Etienne; 1908; Mission Gruvel
MNHN-IM-2022-4603	*Donax rugosus*	Ndiago, beach (16.17°N, 16.51°W)	Articulated specimen with remains of flesh	SacA-68815 $F^{14}C = 0.9376 \pm 0.0022$ (518 ± 19 BP) $\delta^{13}C = 0.68$ ‰ VPDB	January 21st 1908	Mission Gruvel	Donax rugosus Linné, N'Diago plage, 21.I.08, Mission Gruvel

			and hinge ligament.				
Senegal							
MNHN-IM-2022-4607	*Donax rugosus*	Saint Louis (16.02°N, 16.51°W)	Articulated specimen with remains of flesh and hinge ligament.	SacA-68819 $F^{14}C = 0.9310 \pm 0.0021$ (574 ± 18 BP) $\delta^{13}C = 1.29$ ‰ VPDB	December 1901	Mission Buchet	Sénégal, Saint Louis, Coquilles; Donax, M^{on} Buchet, X^{bre} 1901
MNHN-IM-2022-4592	*Senilia senilis*	Dakar, backwaters of the "Marigot de Hann" (14.74°N, 17.39°W)	Articulated specimen with remains of flesh and well-preserved periostracum.	SacA-68824 $F^{14}C = 0.9327 \pm 0.0020$ (560 ± 17 BP) $\delta^{13}C = -0.29$ ‰ VPDB	May 1908	Mission Gruvel	Arca (Senilia) senilis Linné, Marigot de Hann V.1908, se vend sur le marché de Dakar env. 2 sous la douzaine, Mission Gruvel Note: The Marigot of Hann seems to have been a creek more or less connected to the ocean. It was drawn on a map of Dakar in 1905 but does not exist any longer. The map can be accessed from the Gallica website managed by the Bibliothèque Nationale de France: https://gallica.bnf.fr/ark:/12148/btv1b53197802m
MNHN-IM-2022-4593	*Senilia senilis*	Dakar, Bay of Hann, Pointe Bel Air, beach at low tide (14.71°N, 17.42°W)	Articulated specimen with remains of flesh and well-preserved periostracum.	SacA-68825 $F^{14}C = 0.9346 \pm 0.0020$ (544 ± 18 BP) $\delta^{13}C = 0.07$ ‰ VPDB	December 1st 1909	Mission Gruvel	Arca (Senilia) senilis Linné, Baie de Hann, Pointe de Bel Air, plage à basse mer, M Gruvel, 1.XII.1909

MNHN-IM-2022-4606	*Donax rugosus*	Dakar, Bay of Hann (14.71°N, 17.42°W)	Articulated specimen with remains of flesh and hinge ligament.	SacA-68818 $F^{14}C$ = 0.9366 ± 0.0022 (526 ± 18 BP) $\delta^{13}C$ = 0.33 ‰ VPDB	April 1908	Mission Gruvel	Donax rugosus Linné, Baie de Hann à basse mer, IV 08, Mission Gruvel
MNHN-IM-2022-4598	*Bucardium ringens*	Dakar, Bay of Hann at low tide (14.71°N, 17.42°W)	An isolated valve with remains of the hinge ligament.	SacA-68810 $F^{14}C$ = 0.9247 ± 0.0019 (628 ± 17 BP) $\delta^{13}C$ = 0.68 ‰ VPDB	April 1908	Mission Gruvel	Cardium ringens Gmelin, Baie de Hann à basse mer, IV.08, Mission Gruvel
MNHN-IM-2022-4616	*Ostrea stentina*	Dakar, beach of Hann, posts of the pontoon (14.71°N, 17.42°W)	An isolated valve with remains of flesh	SacA-68835 $F^{14}C$ = 0.9351 ± 0.0022 (539 ± 19 BP) $\delta^{13}C$ = 1.56 ‰ VPDB	1947	Roger Sourie	Ostrea stentina Payr Dakar (plage de Hann, piles du ponton) M Sourie 1947
Republic of Guinea							
MNHN-IM-2022-4601	*Bucardium ringens*	Los Islands, Roume Island at low tide (9.46°N, 13.79°W)	Fresh-looking isolated valve.	SacA-68813 $F^{14}C$ = 0.8988 ± 0.0043 (857 ± 39 BP) $\delta^{13}C$ = -0.40 ‰ VPDB	December 20th 1909	Mission Gruvel	Cardium ringens Gmelin; Ile Roumé, archipel de Los, à basse mer, 20.XII.09, Mission Gruvel
MNHN-IM-2022-4618	*Pseudochama gryphina*	Los Islands, Tamara Island (9.46°N, 13.83°W)	Articulated specimen.	SacA-68820 $F^{14}C$ = 0.9395 ± 0.0022 (502 ± 19 BP) $\delta^{13}C$ = 1.52 ‰ VPDB	1909-1910	Mission Gruvel	Chama gryphina Lm, Tamara, Guinée, mission Gruvel, 1909-1910 Note: It is possible that this sample was also collected in December 1909 as sample MNHN-IM-2022-4601
Sierra Leone							
MNHN-IM-2022-4611	*Ostrea stentina*	Near Cape Saint Ann (7.56°N, 12.94°W)	Articulated specimen with remains of flesh.	SacA-68830 $F^{14}C$ = 0.9439 ± 0.0021 (464 ± 18 BP) $\delta^{13}C$ = 1.04 ‰ VPDB	1912	Mission Gruvel	Sierra Léone près Cap Ste Anne, m. Gruvel, 1912
Benin							
MNHN-IM-2022-4591	*Senilia senilis*	Ahémé Lake (6.42°N, 1.96°E)	Articulated specimen with	SacA-68823 $F^{14}C$ = 0.9498 ± 0.0021 (414 ± 18 BP)	February 1910	Mission Gruvel	Arca (Senilia) senilis Linné, Lac Ahémé

			well-preserved periostracum	$\delta^{13}C$ = -4.76 ‰ VPDB			Dahomey, Mission Gruvel, II.1910 Note: Ahémé Lake is located 10 km from the coast, exhibiting only limited connection with the coastal lagoons. Thus, we doubt that this sample is representative of the Atlantic Ocean, and hence we discarded it in our calculation of regional R and ΔR for West Africa.
MNHN-IM-2022-4600	*Bucardium ringens*	Cotonou, dredging at a water depth of 20-25 meters (6.33°N, 2.39°E)	A fresh isolated valve of a juvenile.	SacA-68812 $F^{14}C$ = 0.9273 ± 0.0020 (606 ± 18 BP) $\delta^{13}C$ = 0.26 ‰ VPDB	1910	Mission Gruvel	Cardium ringens, Cotonou, mer, II.1910, sac 372, Mission Gruvel Note: The information that the sample came from a dredging at 20-25 meters water depth in front of Cotonou can be found in Dautzenberg (1912).
MNHN-IM-2022-4602	*Bucardium ringens*	La Bouche du Roi, Grand Popo, beach (6.29°N, 1.92°E)	An isolated valve with remains of the hinge ligament.	SacA-68814 $F^{14}C$ = 0.9365 ± 0.0020 (527 ± 17 BP) $\delta^{13}C$ = 0.25 ‰ VPDB	February 1910	Mission Gruvel	Cardium ringens Gmelin, Bouche du Roi, Gd Popo, plage, II.1910, Mission Gruvel. Note: Three labels mention the same location, but one label mentions the Catumbella estuary (Angola, June 17th 1910). We believe the sample is from Grand Popo.
Ivory Coast							

MNHN-IM-2022-4595	*Bucardium ringens*	Grand Bassam, beach (5.19°N, 3.73°W)	An isolated valve with remains of the hinge ligament.	SacA-68807 $F^{14}C = 0.9388 \pm 0.0021$ (507 ± 18 BP) $\delta^{13}C = 0.29$ ‰ VPDB	1909-1910	Mission Gruvel	Cardium ringens Gmelin, plage de Gd Bassam 1909-10, mission Gruvel.
MNHN-IM-2022-4597	*Bucardium ringens*	Jacqueville, beach (5.19°N, 4.42°W)	An isolated valve of a juvenile with remains of the hinge ligament.	SacA-68809 $F^{14}C = 0.8835 \pm 0.0020$ (995 ± 18 BP) $\delta^{13}C = 0.03$ ‰ VPDB	January 10th 1910	Mission Gruvel	Cardium ringens Gmel., Jacqueville Côte d'Ivoire, plage, 19.I.10, Mission Gruvel.
Gabon							
MNHN-IM-2022-4613	*Ostrea stentina*	Port-Gentil (0.71°S, 8.79°E)	An isolated valve with remains of flesh.	SacA-68832 $F^{14}C = 0.9401 \pm 0.0022$ (497 ± 19 BP) $\delta^{13}C = 2.24$ ‰ VPDB	1948	Charles Roux' mission	Port Gentil, M Roux, 1949. Note: Charles Roux writes in 1949 (Roux, 1949) that he was in the Port-Gentil area during the year 1948. We understand that he was already back in France in 1949. Hence, the Collection date must be 1948 AD.
Republic of Congo							
MNHN-IM-2022-4614	*Ostrea stentina*	Loango (4.66°S, 11.80°E)	An isolated valve with remains of flesh.	SacA-68833 $F^{14}C = 0.9314 \pm 0.0022$ (571 ± 19 BP) $\delta^{13}C = 1.38$ ‰ VPDB	1890	Augusto Nobre	Ostrea stentina Payr Loango M. Nobre 1890
MNHN-IM-2022-4604	*Donax rugosus*	Pointe-Noire (4.76°S, 11.84°E)	A fresh isolated valve from a juvenile specimen.	SacA-68816 $F^{14}C = 0.9459 \pm 0.0021$ (447 ± 18 BP) $\delta^{13}C = 0.84$ ‰ VPDB	December 1936 – April 1937	Edgard Aubert de la Rüe	Pte Noire, Aubert de la Rüe, 1937 Note: Edgard Aubert de la Rüe was in Congo from 18/12/1936 to 16/04/1937 as evidenced by his field books kept in the archives of the Musée du Quai

							Branly (files 2AP/62 to 2AP/64)
Angola							
MNHN-IM-2022-4590	*Senilia senilis*	Cabinda (5.55°S, 12.20°E)	Articulated specimen with well-preserved periostracum.	SacA-68822 $F^{14}C$ = 0.9298 ± 0.0020 (584 ± 17 BP) $\delta^{13}C$ = -1.15 ‰ VPDB	1885-1887	Paul Hesse	Cabinda, Cabinda, Angola; C.R. Boettger coll. 1909 Note: The shell was donated by Caesar R. Boettger to the MNHN in 1909 (Oliver and von Cosel, 1992) but collected earlier by Paul Hesse when Hesse was living in Banana (Democratic Republic of Congo) south of Cabinda (Boettger, 1912). Boettger (1912, p. 110) writes that Hesse's collection includes a number of *Senilia senilis* specimens from Cabinda. The collection date is unfortunately not provided. However, Hesse was employed by a trading company in Banana by the end/beginning 1884/1885 since at least after March 1886 (Westhoff, 1886). Mollusc specimens reported in Boettger (1912) were collected by Hesse between 1885 and 1886. Also, Hesse collected reptile specimens in Cabinda in 1885 and 1887 (Boettger, 1898). Thus, we

							believe that the MNHN specimen must have been collected between 1885 and 1887 AD.
MNHN-IM-2022-4594	*Senilia senilis*	Cabinda (5.55°S, 12.20°E)	An isolated valve with well-preserved periostracum.	SacA-68826 $F^{14}C = 0.9355 \pm 0.0022$ (536 ± 19 BP) $\delta^{13}C = -3.11$ ‰ VPDB	June 6th 1921	Unknown	[Staadt collection]: Arca senilis Lin, Cabenda, Africa, Guinea, bought just over 1d on June 6th 1921 in Grays Jun rd, (some of the specimens at B. M. are more than double the size of mine).
MNHN-IM-2022-4589	*Senilia senilis*	Luanda, beach (8.78°S, 13.27°E)	Articulated specimen with well-preserved periostracum.	SacA-68821 $F^{14}C = 0.9353 \pm 0.0022$ (538 ± 19 BP) $\delta^{13}C = -0.16$ ‰ VPDB	May 18th 1910	Mission Gruvel	Arca (Senilia) senilis Linné, St Paul de Loanda, plage, Mission Gruvel, 18.V.1910.
MNHN-IM-2022-4605	*Donax rugosus*	Luanda, beach (8.82°S, 13.21°E)	Articulated specimen with remains of flesh and hinge ligament.	SacA-68817 $F^{14}C = 0.9364 \pm 0.0021$ (528 ± 18 BP) $\delta^{13}C = 0.82$ ‰ VPDB	May 18th 1910	Mission Gruvel	Donax rugosus Linné, St Paul de Loanda plage, 18.V.10, Mission Gruvel.
MNHN-IM-2022-4596	*Bucardium ringens*	Bay of Lobito, near the peninsula (12.33°S, 13.56°E)	An isolated valve.	SacA-68808 $F^{14}C = 0.9286 \pm 0.0020$ (595 ± 17 BP) $\delta^{13}C = 1.51$ ‰ VPDB	June 1910	Mission Gruvel	Cardium ringens Gmelin, Baie de Lobito côté presqu'île, VI.1910, mission Gruvel.
MNHN-IM-2022-4617	*Ostrea stentina*	Moçâmedes (15.18°S, 12.14°E)	A fresh isolated valve.	SacA-68836 $F^{14}C = 0.9317 \pm 0.0021$ (568 ± 18 BP) $\delta^{13}C = 1.75$ ‰ VPDB	1910	Mission Gruvel	Mossamédès, m Gruvel, 1910